BULLETIN OF STOMATOLOGY AND MAXILLOFACIAL SURGERY
Volume 20, Issue 1

DOI: 10.58240/1829006X-2024.1-111

RESEARCH ARTICLE

ANALYSIS OF SKIN SCARRING WITH PRE-, INTRA- AND DELAYED SURGICAL INJECTION THERAPY: THE PRECLINICAL RESEARCH

Olga Danishchuk MD,[1*] Aleksey Volkov MD, DSc,[2] Vladimir Reshetin MD,[3] Marina Danishchuk MD,[4] Elena Karpova MD, DSc,[5] David Nazarian MD, DSc[6]

1. Research assistant, "Danishchuk Clinic", Department of Plastic and Aesthetic Surgery of the Academy of Postgraduate Education FGBU FSCC FMBA of Russia, Moscow, RF
2. Department of anatomical pathology, St. Alexius Hospital, Moscow, Russia
3. Department of anatomical pathology, Hospital for War Veterans № 2, Moscow, RF
4. Danishchuk Clinic, Moscow, RF
5. Professor, Department of Skin Diseases and Cosmetology, Pirogov Russian National Research Medical University, Moscow, Russia
6. Professor, Department of Plastic and Aesthetic Surgery of the Academy of Postgraduate Education FGBU FSCC FMBA of Russia, Moscow, RF

** Corresponding author: Danishchuk Olga, Lukov Lane, 4, Moscow, RF, 107045, Phone: +7 9031072208; e-mail: danolga@mail.ru*

Received: *Jan 12, 2024;* ***Accepted:*** *Mar 13, 2024;* ***Published:*** *Mar 25, 2024*

Abstract

Purpose: Experimental testing of injection therapy in the area of the upcoming skin incision in order to improve the quality of achieving the aesthetic appearance of the skin scarring process.

Materials and methods: The study was carried out on the skin of the sternum and anterior abdominal wall on 2 closely related minipigs.3 series of operations were carried out synchronously on two individuals in a surgical operating room with preliminary specific markings in the form of rectangles and trapezoids, respectively; the nipple-areolar complexes served as a guide for drawing the figures. At each stage, the same type of geometric marking of the surgical field was used and repeated interventions were performed in the same areas of injection therapy and biopsy sampling. In the postoperative period, on the 30th and 120th days, biopsy specimens were taken to verify the ongoing reparative processes based on clinical, photometric and histological analysis.

Results: Preoperative injection therapy contributed to the formation of a normotrophic scar in structure closer to normal skin compared to a scar during normal tissue healing, which allows it to be recommended for preoperative preparation and for research in humans. The selected technique allows for assessment of the classic primary wound, with the introduction of saline and botulinum toxin intraoperatively and delayed at 1 and 4 months with histological analysis of the results. At each stage of the experiment, the team achieved long-term survival of minipigs without compromising their vital functions. The same type of geometric marking of the surgical field was used and repeated interventions were performed in the same areas of injection therapy and biopsy sampling.

Conclusion: The methodology allows to assess different methods of linear scar formation with or without the use of injection therapy during surgical access, as well as comparing tissue adhesion histologically and optimal scar formation. When the effectiveness of BTA therapy is achieved, injection therapy requires further research under conditions of tissue deficit or tension during wound closure.

Keywords: *botulinum toxin; relatox; bta; scar; pathological scar; prevention of pathological scarring; hypertrophic scar; keloid; keloid scar.*

Introduction

The restoration of deformed tissues and lost organs of the human body has always been relevant in the range of medical and social problems of mankind. Injuries to the head and neck are particularly difficult to achieve functional and cosmetic restoration.[1,2]

Extensive cicatricial deformations of the skin on the face greatly disfigure the appearance, leaving both patients and operating surgeons dissatisfied with the results of treatment.[3]

Recent decades have been characterized by significant progress in the development of plastic, reconstructive and cosmetic surgery.[4]

This is explained by advances in transplantology, new discoveries in morphology, and the introduction of modern biotechnologies and microsurgical methods.[5] Today, there are many methods and techniques aimed at improving the appearance of the scar and the quality of life of patients in general, but very little research has been aimed at studying the prevention of scar formation.[6]

The article describes an experimental study carried out to analyse skin scarring during formation and closure of wounds using various injections in surgical access sites. Previously, we have described known methods for preventing pathological scarring of the skin in our narrative review. The team reviewed, reviewed the available literature and applied various types of injection therapy in order to identify the most optimal drug for improving the skin scar.[7]

It should be noted that the chosen experimental technique is unique both in its complexity of synchronous work of two surgical teams, and in the fact that in the future this experiment can serve as a method for training surgeons in other disciplines using online cameras and monitors. An important advantage of this technique is the humaneness of the experiment, in which the lives of both individuals are preserved.

The most popular biological model for performing experimental work in surgery is the laboratory mouse. In our work, we tested the technique on minipigs as a biological experimental model, and achieved positive results in the form of adhesion of wound edges and taking similar biopsies at various time intervals, recording the results clinically, photometrically and histologically.

The aim of this study is to improve the quality of life of the living organism undergoing surgical intervention with skin excision, by testing and selecting the optimal pre-, intra-, and post-operative method of injection therapy and achieving an optimal aesthetic-functional result of scar formation.

Objectives

1. To analyse the effectiveness of injection therapy in the surgical access area and to improve the aesthetic-functional outcome of scars formation.
2. To achieve the survival of all individuals during the experiment
3. To develop anaesthesia protocols for laboratory animals/mini-pigs.
4. To conduct evidence-based analysis using photometry and histological examination.

Thus, the experiment was conducted to verify the hypothesis - do modern injection therapy improves or worsens the scarring process.

Materials and methods

3 series of surgical intervention on two closely related minipigs (24 months, weighing 45 kg) were held during the experiment. The authors selected minipigs for this experiment based on their successful experience achieved during cross-transplantation of face on minipigs from 2016 to 2019 (Figure 1).

Figure 1. *Minipigs after cross-transplantation of face*

The surgical intervention was carried out simultaneously on two individuals in an operating

theatre room using standard surgical set. During the postoperative period, biopsies were taken at 30 and 120 days to analyse ongoing reparative mechanisms. Photography and biopsy sampling were performed at all stages of the experiment. Various types of injection therapy were considered and applied to identify the most optimal drug for optimal scars formation. The initial stage of surgical experiment was held on November 3, 2022 under intravenous sedation with the participation of a veterinary anesthesiologist and 4 surgeons. Both teams synchronously marked along the nipple-areolar complexes a rectangle on the thoracic area and a trapezium in the area of the anterior abdominal wall. The minipigs had code numbers 955 and 957. In minipig N955, a biopsy sample measuring 1x1 cm was taken from a rectangular marked area without injections, and the wound was sutured without tension with Vicryl 4.0. From the same minipig, a 1x1 cm biopsy sample was taken from the area of the anterior abdominal wall 15 minutes after the injection of 2 ml of saline. The wound was sutured without tension in the same manner. In minipig N957, in the projection of a rectangular marking, a 1x1 cm biopsy sample was taken 15 minutes after the injection of 2 ml of BTA solution. At the same time in the projection of the anterior abdominal wall, 2 ml of BTA solution was administered for delayed biopsy collection. In total, at the first stage, 3 biopsies were taken (see Figure 2).

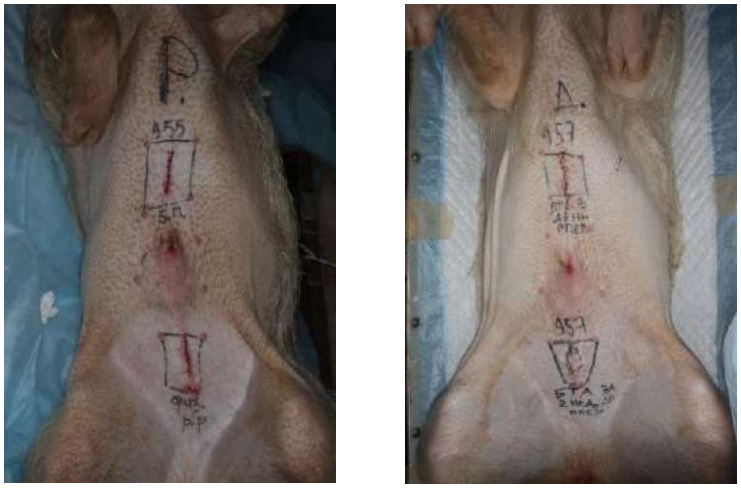

Figure 2. *The initial stage of surgical experiment (November 3, 2022): Injection of toxin and skin defect formation and suturing.* ***A*** *- minipig N955. Rectangle – biopsy was taken (control group). Trapezium - biopsy was taken 15 minutes after the injection of saline.* ***B*** *- minipig N957. Rectangle - biopsy sample was taken 15 minutes after the injection of BTA solution. Trapezium - BTA solution was administered for delayed biopsy collection*

The second stage of the experiment was performed on December 8, 2022. Under intravenous sedation with the participation of a veterinary anesthesiologist. Both teams, in the same manner as at the previous stage, marked along the nipple-areolar complexes a rectangle on the thoracic area and a trapezium in the area of the anterior abdominal wall.

In minipig N955, no biopsy sample was taken from the rectangular marked area during the second stage. However, a repeat 1x1 cm biopsy was taken from the area of the anterior abdominal wall, previously injected with saline. The wound was sutured without tension with Vicryl 4.0.

In minipig N957, a repeat biopsy was taken from the rectangular marking area. Additionally, a primary 1x1 cm biopsy was taken from the anterior abdominal wall after 35 days of BTA injection for further delayed investigation of tissue reparation.

In total, at the second stage, 3 biopsies were taken (see Figure 3).

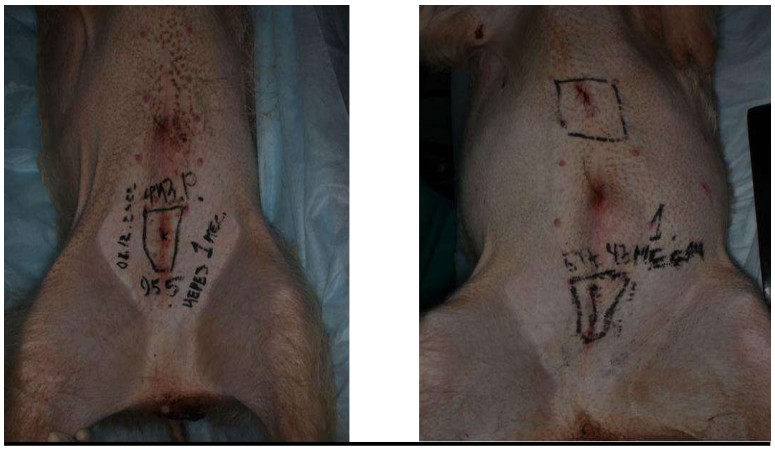

Figure 3. *Second stage of the experiment (December 8, 2022).* ***A*** *- minipig N955. A repeat biopsy was taken from the area of the anterior abdominal wall, previously injected with saline.* ***B*** *- minipig N957. Rectangle - repeat biopsy was taken Trapezium - a primary biopsy was taken*

The third stage of surgical experiment was held on March 3, 2023. The marking principle remained the same.

In minipig N955, a biopsy sample measuring 1x1 cm was taken from a rectangular marked area. And a 1x1 cm biopsy sample was taken from the area of the anterior abdominal wall.

In minipig N957, in the projection of a rectangular marking, a 1x1 cm biopsy sample was taken from a rectangular marked area. At the same time in the projection of the anterior abdominal wall, a secondary biopsy measuring was taken after 120 days of BTA injection.

In total, at the third stage, 4 biopsies were taken (see Figure 4).

Figure 4. *Third stage of the experiment (March 3, 2023).* ***A*** *- minipig N955. Rectangle - repeat biopsy was taken. Trapezium - a repeat biopsy was taken.* ***B*** *- minipig N957. Rectangle - repeat biopsy was taken Trapezium - a secondary biopsy was taken*

In total, 10 biopsy specimens were taken during all three stages. In this study, the BTA drug "Relatox" ("NPO Microgen", Russia) and saline "Solopharm" ("Grotesk" Russia) were used at all 3 stages.

During postoperative period, experimental animals received antibacterial (interspectin IM single injections 1 ml/10kg) for 14 days to prevent secondary bacterial infection. The collection of specimens for histological examination on days 30 and 120 was carried out under intravenous sedation using Zoletil-100 1.5 mg/kg and Xyla 0.15 ml/kg.

Results

See Table 1 and the scheme of interventions on minipigs, as well as time intervals, are presented in Figure 5.

Table 1. *Realization of scar models with and without injection therapy at various stages of the experiment*

Number of specimen	Number of specimens	Number of biopsies taken	Design of the experiment
I stage - initial interventions			
2	4	3	biopsy without injection biopsy with intraoperative saline injection biopsy with intraoperative BTA injection preoperative BTA injection
II Stage - after 1 month			
2	4	3	repeat biopsy with intraoperative saline injection repeat biopsy with intraoperative BTA injection primary preoperative BTA injection
III Stage - after 4 months			
2	4	4	repeat biopsy without injection repeat biopsy with intraoperative saline injection repeat biopsy with intraoperative BTA injection repeat preoperative BTA injection
In Total: 2	In Total: 12	In Total: 10	

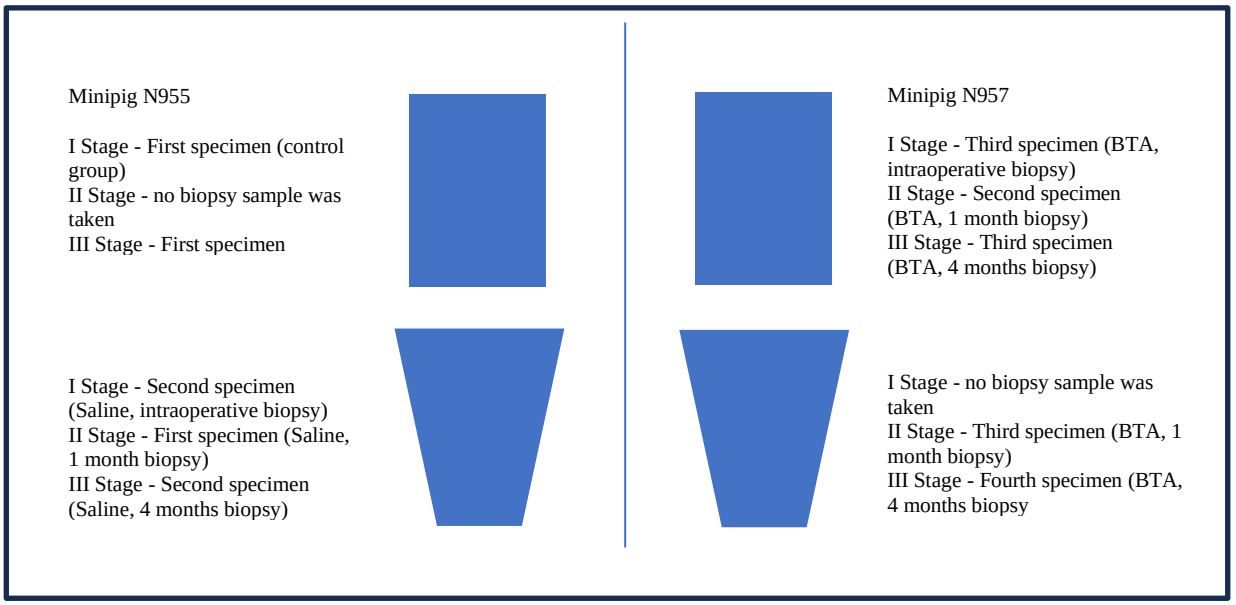

Figure 5. *A conventional diagram of experimental specimens' markings, used in all 3 stages to maintain the accuracy of the injections and surgical incisions*

Histological analysis Stage I (3 yellow samples)

Description of the first specimen

Skin fragments are represented by a stratified squamous epithelium with usual structure. The epithelium has outgrowths and folds of various sizes. The folds of the epidermis are smoothed, their height is reduced. All 5 sublayer of epidermis (stratum basale, spinosum, granulosum, lucidum, corneum) are clearly identified. The keratinization is well expressed. The thickness of the epithelium is noticeably less than dermis (Figure 6).

Figure 6. *Histopantomogram. A fragment of skin. Thin epidermis and thick dermis. Mallory staining. Magnification 3x*

The structure of the dermis is heterogeneous, with areas of uneven thickness of collagen fibers. In the central part, collagen fibers of medium thickness and moderate cellularity are observed. Blood-filled capillaries are represented between the fibers. The fibers are densely arranged, but with reduced retraction phenomenon. Fiber bundles within the central zone are of comparable size and moderate density. Metachromasia demonstrates moderate and equal compaction of collagen fibers within the densely fibrous connective tissue. At the periphery of the described area, collagen fibers with larger diameter are observed (Figure 7).

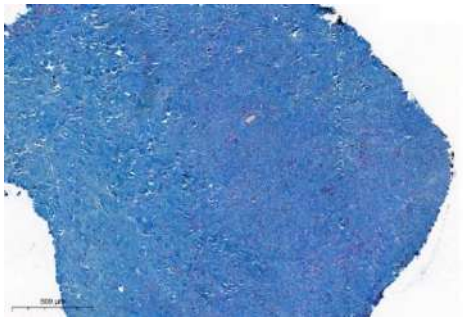

Figure 7. *A fragment of skin. The folds of the epidermis are smoothed, their height is reduced. Mallory staining. Magnification 100x*

Picro-sirius red staining revealed clear predominance of collagen type I over collagen type III. Collagen fibrils in bundles of densely fibrous connective tissue show predominantly red fluorescence (Figure 8).

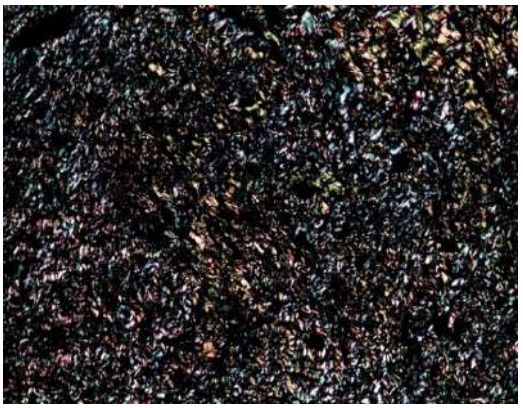

Figure 8. *A fragment of skin. The folds of the epidermis are smoothed, their height is reduced. Picro-sirius red staining. Magnification 50x*

Description of the second specimen

Skin fragments are represented by a stratified squamous epithelium with usual structure. The epithelium has outgrowths and folds of various sizes. The folds of the epidermis are smoothed, their height is reduced. All 5 sublayer of epidermis (stratum basale, spinosum, granulosum, lucidum, corneum) are clearly identified. The keratinization is well expressed. The thickness of the epithelium is noticeably less than dermis (Figures 9, 10).

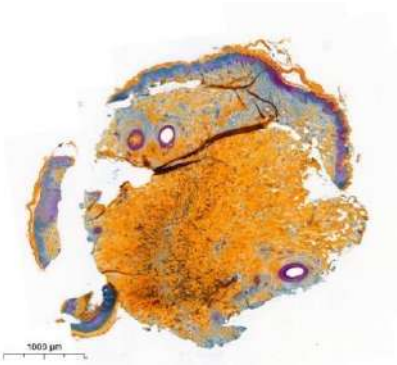

Figure 9. *Histopantomogram. A fragment of skin. Thin epidermis and thick dermis with dense compaction of collagen fibers (thick scar). Mallory staining. Magnification 3x*

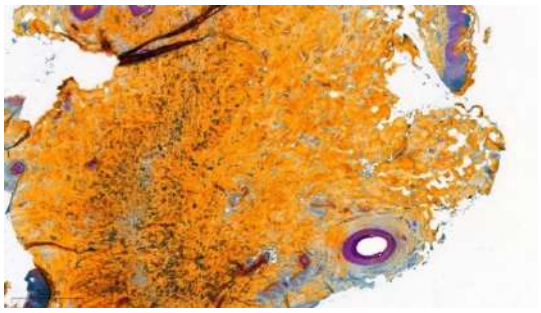

Figure 10. *A fragment of skin. Dense bundles of collagen fibers are brightly dyed. Mallory staining. Magnification 100x*

The structure of the dermis is heterogeneous contains. Also, the areas with a high density of collagen fibers are clearly identified. Metachromasia demonstrates a pronounced deposition of collagen fibers (yellow staining). Blue-stained collagen fibers with smaller diameter are observed at the periphery (Figure11).

Figure 11. *A fragment of skin. Anisotropic red fluorescence in the central zone of the samples. Picro-sirius red staining. Magnification 50x*

Picro-sirius red staining revaled clear predominance of collagen type I over collagen type III. As in previous sample, Collagen fibrils in bundles of densely fibrous connective tissue show predominantly red fluorescence

Description of the third specimen

This sample is represented by stratified squamous epithelium and subcutaneous fat (Figures 12, 13).

Figure 12. *Histopantomogram. A fragment of skin. Thin epidermis and thick dermis. Mallory staining. Magnification 3x*

The epithelium has outgrowths and folds of various sizes. The folds of the epidermis are smoothed, their height is reduced. All 5 sublayer of epidermis (stratum basale, spinosum, granulosum, lucidum, corneum) are clearly identified. The keratinization is well expressed. The thickness of the epithelium is noticeably less than dermis (Figures 9, 10).

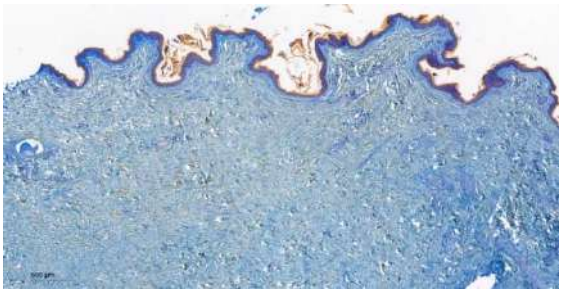

Figures 13. *A fragment of skin. The folds of the epidermis are smoothed, their height is reduced*

The densely arranged bundles of connective tissue fibers, with reduced retraction phenomenon. Moderate compaction of collagen Mallory staining. Magnification 100x

The dermis is represented by fibrous, irregular connective tissue with areas of dense bundles of collagen fibers, originating from the epidermis and extending deep into the dermis. Mallory's aniline blue staining revealed the densely arranged bundles of connective tissue fibers, with reduced retraction phenomenon. Metachromasia demonstrates moderate compaction of collagen fibers in bundles within densely fibrous irregular connective tissue in the central part of the samples.

Picro-sirius red staining revaled a predominant expression of collagen type I over collagen type III. Evaluation of the anisotropic fluorescence distribution of collagen fibers in samples from this group demonstrated a even increase in collagen type I (red and yellow fluorescence) in the central part of the dermis samples, while the distribution of collagen types I and III was regular only at the edges of the samples (Figure 13).

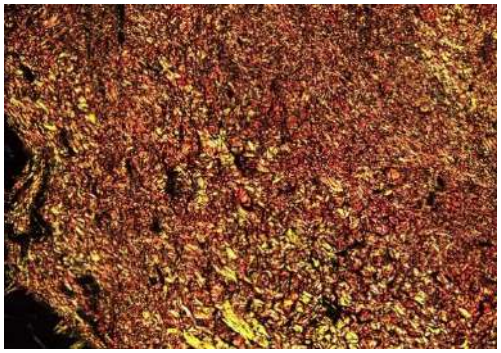

Figure 14. *A fragment of skin. Anisotropic red fluorescence in the central zone of the samples. Picro-sirius red staining. Magnification 50x*

Evaluation of the anisotropic fluorescence distribution of collagen fibers in samples from this group demonstrated an even increase in collagen type I (red and yellow fluorescence) in the central part of the dermis, while the distribution of collagen types I and III was regular only at the edges of the samples.

Thus, a comparative analysis of samples from the first series (biopsy collection on 03.11.2022) did not reveal significant differences between sample 1 and sample 3 in the quantity and quality of collagen types I and III distribution. Sample 2 showed a significant accumulation of dense collagen fibers (the reason for densification is unclear) The structure of the dermis in samples 1, 2, and 3 showed little differences. Although, in sample 3, collagen fibers in the central part of the dermis are thickened and have a nodular structure.

Stage II (3 green samples)

Description of the first specimen

The sample is represented by stratified squamous epithelium and subcutaneous fat (Figure 15).

Figure 15. *Histopantomogram. A fragment of skin. Thin epidermis and thick dermis. Mallory staining. Magnification 3x*

The epithelium has outgrowths and folds of various sizes. All 5 sublayer of epidermis (stratum basale, spinosum, granulosum, lucidum, corneum) are clearly identified. The keratinization is well expressed. The thickness of the epithelium is noticeably less than dermis (Figure 16).

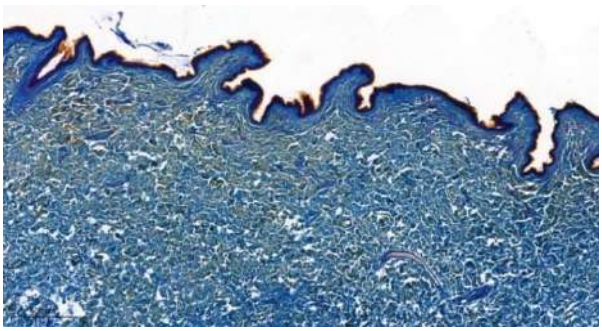

Figure 16. *A fragment of skin. Thin epidermis Mallory staining. Magnification 3x*

The dermis is represented by fibrous, irregular connective tissue. Mallory's aniline blue staining revealed the loosely arranged bundles of connective tissue fibers, with reduced retraction phenomenon. Metachromasia demonstrates moderate compaction of collagen fibers in bundles.

Picro-sirius red staining revealed equal distribution of types I and III collagen. Collagen fibrils of dense connective tissue simultaneously show green, yellow and, to a lesser extent, red fluorescence (Figure 17).

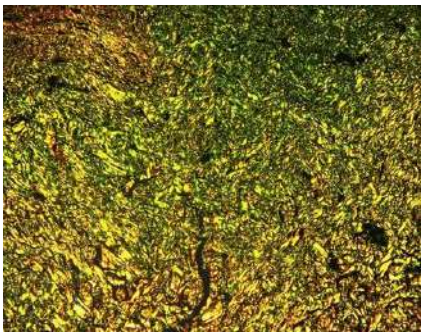

Figure 17. *A fragment of skin. Progressive growth of type I collagen from the superficial layers of the dermis to deeper. Type III collagen – green fluorescence. Type I collagen – yellow and red fluorescence. Picro-sirius red staining. Magnification 50x*

Evaluation of the anisotropic fluorescence distribution of collagen fibers in samples from this group demonstrated a hierarchical, progressive increase of collagen type I from the superficial layers of the dermis to the deeper layers. And at the same time, a corresponding decrease of collagen type III is observed. The increase of collagen type III occurs within the bundles of collagen fibers.

Description of the second specimen

The sample is represented by stratified squamous epithelium and subcutaneous fat (Figure 18).

Figure 18. *Histopantomogram. A fragment of skin. Thin epidermis and thick dermis. Mallory staining. Magnification 3x*

The epithelium has outgrowths and folds of various sizes. The folds of the epidermis are smoothed, their height is reduced. All 5 sublayer of epidermis (stratum basale, spinosum, granulosum, lucidum, corneum) are clearly identified. The keratinization is well expressed. The thickness of the epithelium is noticeably less than dermis (Figure 19).

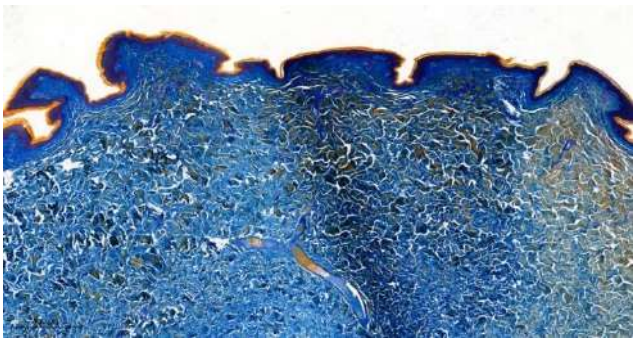

Figure 19. *A fragment of skin. The folds of the epidermis are smoothed, their height is reduced. Mallory staining. Magnification 100x*

The dermis is represented by fibrous, irregular connective tissue with areas of dense bundles of collagen fibers, originating from the epidermis and extending deep into the dermis. Mallory's aniline blue staining revealed the densely arranged bundles of connective tissue fibers, with reduced retraction phenomenon. But their distribution is not equal, with a greater localization around fibers with a yellowish-reddish staining, which correspond to denser fibers. Metachromasia demonstrates moderate compaction of collagen fibers in bundles at the edges of the sample, while in the central zone compaction is slightly reduced.

Picro-sirius red staining revealed uneven distribution of types I and III collagen. Thus, collagen fibrils of dense connective tissue are shown predominantly in the central area of the samples (red fluorescence). Meanwhile, the predominance of yellow fluorescence is mainly at the edges of the samples (Figure 20).

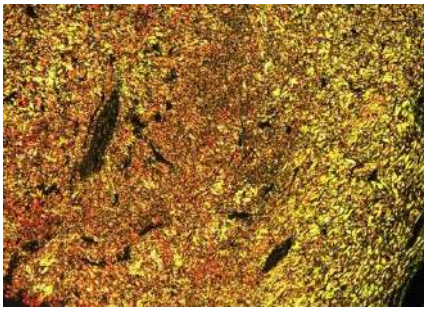

Figure 20. *A fragment of skin. Anisotropic red fluorescence in the central zone of the samples. Picro-sirius red staining. Magnification 50x*

Evaluation of the anisotropic fluorescence distribution of collagen fibers in samples from this

group demonstrated an uneven increase in collagen type I (red and yellow fluorescence) in the central part of the dermis samples. In turn, the distribution of type I and III collagen was regular only at the edges of the samples (Figure 21).

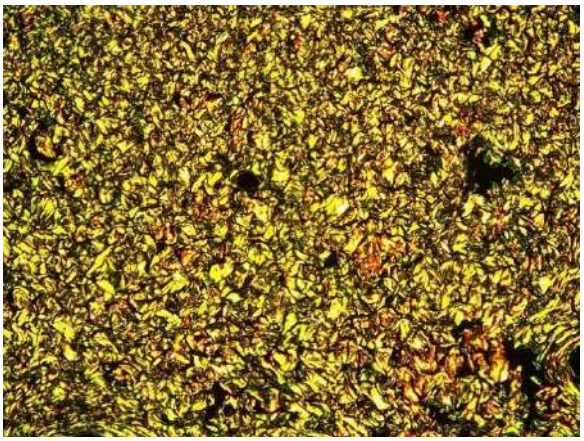

Figure 21. *A fragment of skin. The distribution of type I and III collagen was regular only at the edges of the samples. Picro-sirius red staining. Magnification 10x*

Description of the third specimen

The sample is represented by stratified squamous epithelium and subcutaneous fat (Figure 22).

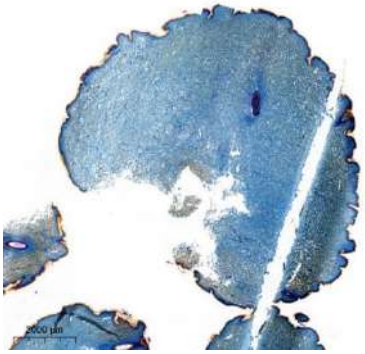

Figure 22. *Histopantomogram. A fragment of skin. Thin epidermis and thick dermis. Inside the dermis the outgrowth of collagen fibers with a low compaction is observed. Mallory staining. Magnification 1,5x*

The epithelium has outgrowths and folds of various sizes. The folds of the epidermis are smoothed, their height is reduced. All 5 sublayer of epidermis (stratum basale, spinosum, granulosum, lucidum, corneum) are clearly identified. The keratinization is well expressed. The thickness of the epithelium is noticeably less than dermis (Figure 23).

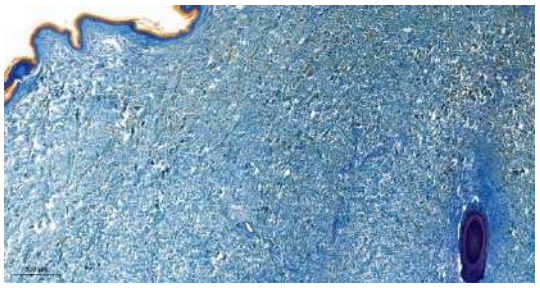

Figure 23. *Histopantomogram. A fragment of skin. Moderate density of connective tissue fibers is observed Mallory staining. Magnification 100x*

The dermis is represented by dense, irregular connective tissue with areas of loose bundles of collagen fibers, originating from the epidermis and extending deep into the dermis. Mallory's aniline blue staining revealed equal distribution of connective tissue fibers. Metachromasia demonstrates low compaction of collagen fibers in bundles at the edges of the sample, while in the central zone compaction is slightly reduced.

Picro-sirius red staining revealed equal and moderate distribution of types I and III collagen. Thus, collagen fibrils of dense connective tissue are shown predominantly in the central area of the samples (yellow and green fluorescence). Meanwhile, the predominance of red fluorescence is mainly at the edges of the samples (Figure 24).

Figure 24. *A fragment of skin. Anisotropic red fluorescence in the central zone of the samples. Picro-sirius red staining. Magnification 10x*

A comparative analysis of samples of the second stage of the experiment revealed that in first specimen there is an uneven distribution and uneven maturity of collagen, both within individual bundles and on the scale of the dermis. In turn, in second specimen there is a predominance of type I collagen in the central part of the sample, which may indicate

the absence of the effect of BTA directly during surgery. In turn, in sample No. 2 there is a predominance of type I collagen in the central part of the sample, which may indicate the absence of direct effect of BTA. Whereas in third specimen, the distribution of collagen with low compaction was observed in the central part of the sample, which indicates the benefits of delayed BTA injection.

Stage III (4 purple samples)

Description of the first specimen

Skin fragments are represented by a stratified squamous epithelium with usual structure. The epithelium has outgrowths and folds of various sizes. The folds of the epidermis are smoothed, their height is reduced. All 5 sublayer of epidermis (stratum basale, spinosum, granulosum, lucidum, corneum) are clearly identified. The keratinization is well expressed. The thickness of the epithelium is noticeably less than dermis (Figures 25, 26).

Figure 25. *Histopantomogram. A fragment of skin. Thin epidermis and thick dermis. Inside the dermis the outgrowth of collagen fibers is observed. Mallory staining. Magnification 1,5x*

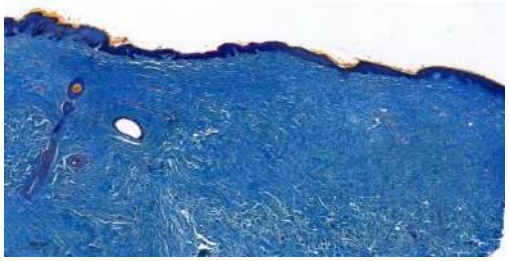

Figure 26. *A fragment of skin. The folds of the epidermis are smoothed, their height is reduced. Low uneven compaction of collagen fibers within dense connective tissue is observed over the entire area of the samples Mallory staining. Magnification 100x*

In the second specimen, the dermis is not homogeneous; there are areas with uneven thickness of collagen fibers. The collagen fibers of dense fibrous connective tissue with medium thickness and low cellularity are observed throughout the entire area of the sample. Blood-filled capillaries are represented between the fibers. The retraction phenomenon is uneven. Some fiber bundles have undergone retraction, while others retained their compact structure. Metachromasia demonstrates low uneven compaction of collagen fibers within dense connective tissue over the entire area of the samples (Figure 27).

Figure 27. *A fragment of skin. Regular, anisotropic fluorescence of type I and type III collagens. Picro-sirius red staining. Magnification 50x*

Picro-sirius red staining revealed an uneven predominance of collagen type I over collagen type III. The collagen fibrils of dense connective tissue have predominantly yellowish-red fluorescence.

Description of the second specimen

Skin fragments are represented by a stratified squamous epithelium with usual structure. The epithelium has outgrowths and folds of various sizes. The folds of the epidermis are smoothed, their height is reduced. All 5 sublayer of epidermis (stratum basale, spinosum, granulosum, lucidum, corneum) are clearly identified. The keratinization is well expressed. The thickness of the epithelium is noticeably less than dermis (Figures 28, 29).

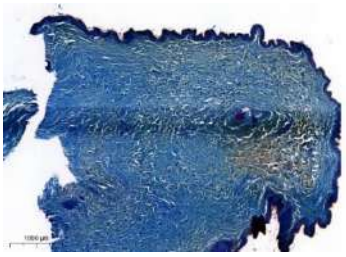

Figure 28. *Histopantomogram. A fragment of skin. Thin epidermis and thick dermis. Metachromasia demonstrates low uneven compaction of collagen fibers within dense fibrous connective tissue over the entire area of the samples. Mallory staining. Magnification 1,5x*

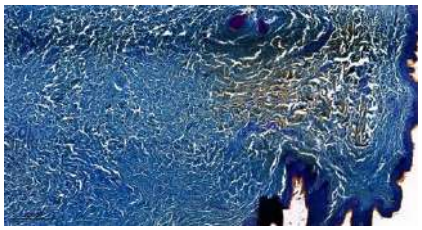

Figure 29. *A fragment of skin. The folds of the epidermis are smoothed, their height is reduced. Bundles of connective tissue fibers are compacted in a small area of the sample. Mallory staining. Magnification 100x*

The dermis is homogeneous with high compaction of collagen fibers at the centre. The collagen fibers of dense fibrous connective tissue with medium thickness and low cellularity are observed throughout the entire area of the sample. Blood-filled capillaries are represented between the fibers. The retraction phenomenon is even and well expressed. Metachromasia demonstrates low uneven compaction of collagen fibers within dense fibrous connective tissue over the entire area of the samples, except for a small area in the centre of the sample (Figure 30).

Figure 30. *A fragment of skin. Regular, anisotropic fluorescence of type I and type III collagens. Picro-sirius red staining. Magnification 100x*

Picro-sirius red staining revealed an uneven predominance of collagen type I over collagen type III. The collagen fibrils of dense connective tissue have predominantly yellowish-red and greenish fluorescence.

Description of the third specimen

Skin fragments are represented by a stratified squamous epithelium with usual structure. The epithelium has outgrowths and folds of various sizes. The folds of the epidermis are smoothed, their height is reduced. All 5 sublayer of epidermis (stratum basale, spinosum, granulosum, lucidum, corneum) are clearly identified. The keratinization is well expressed. The thickness of the epithelium is noticeably less than dermis (Figures 31, 32).

Figure 31. *Histopantomogram. A fragment of skin. Thin epidermis and thick dermis. Metachromasia demonstrates low uneven compaction of collagen fibers within dense fibrous connective tissue over the entire area of the samples. Mallory staining. Magnification 1,5x*

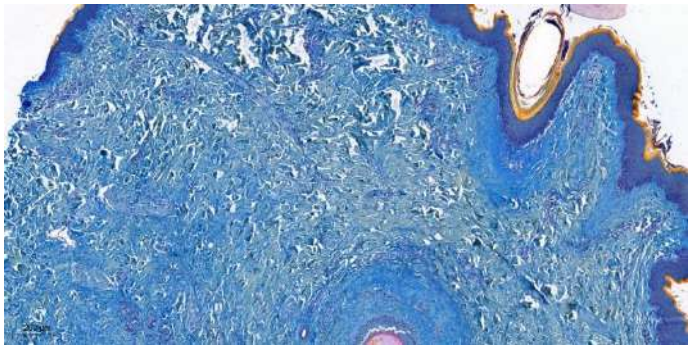

Figure 32. *A fragment of skin. The folds of the epidermis are smoothed, their height is reduced. Bundles of connective tissue fibers are compacted in a small area of the sample. Mallory staining. Magnification 100x*

The dermis is homogeneous with high compaction of collagen fibers at the centre. The collagen fibers of dense fibrous connective tissue with medium thickness and low cellularity are observed throughout the entire area of the sample. Blood-filled capillaries are represented between the fibers. The retraction phenomenon is even and well expressed. Metachromasia demonstrates low uneven compaction of collagen fibers within dense fibrous connective tissue over the entire area of the samples, except for a small area in the centre of the sample.

Picro-sirius red staining revealed an uneven predominance of collagen type I over collagen type III. The collagen fibrils of dense connective tissue have predominantly yellowish-red fluorescence.

Description of the fourth specimen

Skin fragments are represented by a stratified squamous epithelium with usual structure. The epithelium has outgrowths and folds of various sizes. The folds of the epidermis are smoothed, their height is reduced. All 5 sublayer of epidermis (stratum basale, spinosum, granulosum, lucidum, corneum) are clearly identified. The keratinization is well expressed. The thickness of the epithelium is noticeably less than dermis (Figures 33, 34).

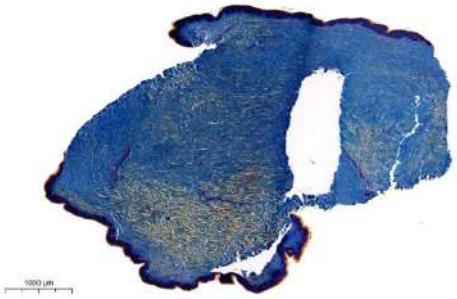

Figure 33. *Histopantomogram. A fragment of skin. Thin epidermis and thick dermis. The dermis is heterogeneous with clearly distinguished two layers. Mallory staining. Magnification 3x*

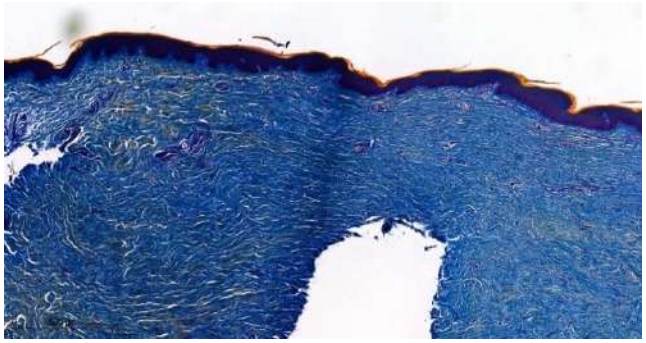

Figure 34. *Histopantomogram. A fragment of skin. Thin epidermis and thick dermis. The dermis is heterogeneous with clearly distinguished two layers. Mallory staining. Magnification 100x*

The dermis is heterogeneous with clearly distinguished two layers. The zone located directly under the epithelium consists of collagen fibers with a larger diameter compared to those located below, visually forming the second zone. The superficial layer consists of collagen fibers having a larger diameter than those located below. The collagen fibrils of dense fibrous connective tissue with medium thickness and low cellularity observed throughout the entire layer. Blood-filled capillaries are represented between the fibers. The retraction phenomenon is even and well expressed. Metachromasia demonstrates low equal compaction of collagen fibers within dense fibrous connective tissue over the entire area of superficial layer.

In the lower layer, the thickness of collagen fibers is approximately half that of the superficial layer. The retraction phenomenon is weakly expressed. The fibers have moderate cellularity and stained well with blue dye (Figure 35).

Figure 35. *A fragment of skin. Regular, anisotropic fluorescence of type I and type III collagens. The collagen fibrils of dense connective tissue have predominantly yellowish-red fluorescence. Picro-sirius red staining. Magnification 100x*

Picro-sirius red staining revealed an uneven predominance of collagen type I over collagen type III. The collagen fibrils of dense connective tissue have predominantly yellowish-red fluorescence.

Analysing samples of series 3, the formation of a thick scar was revealed in first and second specimens. It's obviously explained by predominance of type 1 collagen at the site of surgical damage. In contrast, third and fourth specimens showed an equal distribution of type I and type III collagen, which somewhat similar to first specimen of Series 1. It is worth noting that the distribution of type I and type III collagens in fourth specimen is closest to natural ratio.

This experimentally validated method is an option for planned or delayed surgical interventions in patients predisposed to pathological scarring. And this experiment can be considered as a preclinical testing before clinical trials (Fig. 36, 37, 38)

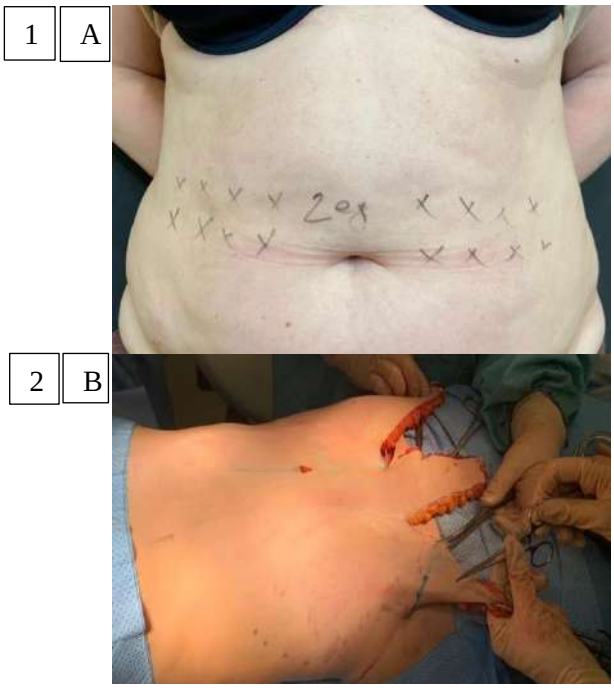

Figure 36. *Preliminary clinical trials* ***1)*** *Marking in the projection of the surgical incision 14 days before abdominoplasty:* ***A*** *– using BTA /* ***B*** *– using saline solution.* ***2)*** *Skin flap elevation during abdominoplasty*

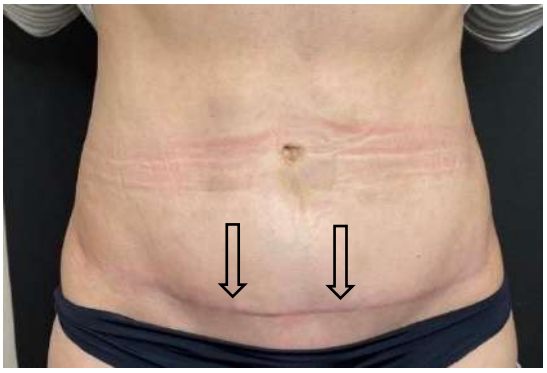

Figure 37. Clinical outcome postoperatively

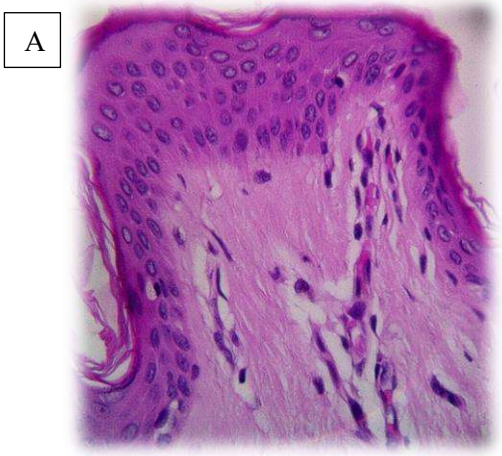

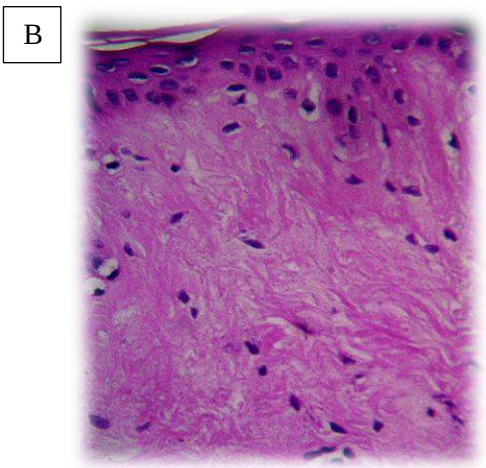

Figure 38. *Histological analysis of skin samples 14 days after administration of BTA* ***(A)*** *and saline* ***(B)***

Analysing the morphological data, obtained during experiment, it was found that the relief and the thickness of the epidermis and the papillary layer of the dermis are similar in the experimental and control samples. However, the thickness of the reticular layer of the dermis in experimental samples is significantly superior to the control group, which may determine the greater density of the skin. At the same time, the structure of the collagen fibers in reticular layer of the dermis does not differ in both groups.

Furthermore, differences in the papillary layer of the dermis were also found. The oedema in experimental group is less expressed, the collagen fibers are better structured, and significantly more capillaries are present in the papillary layer of the dermis. Wherein, the composition and structure of glycosaminoglycans in the experimental and control samples remained the same. This indicates better blood supply and less expressed sclerotic changes of the papillary layer in the experimental sample.

Final conclusion

Preoperative injection therapy contributes the formation of a normotrophic scar structurally closer to normal skin compared to a scar with conventional tissue healing. This preliminary research allows to recommend this methodology for clinical trials development and further patients preoperative preparation.

Declarations

Conflicts of interest and financial disclosures

The author declares that he has no conflict percent and there was no external source of funding for the research in question.

Ethical approval

The research related to animals' use has been complied with all the relevant national regulations and institutional policies for the care and use of animals

Source of funding

This research received no external funding.

Data Availability Statement

Not applicable.

REFERENCES

1. Fu XB. Repair cell first, then regenerate the tissues and organs. *Mil Med Res*. 2021;8(1):2. doi:10.1186/s40779-021-00297-5
2. Krafts KP. Tissue repair: The hidden drama. *Organogenesis*. 2010;6(4):225-33. doi:10.4161/org.6.4.12555
3. Honigman RJ, Phillips KA, Castle DJ. A review of psychosocial outcomes for patients seeking cosmetic surgery. *Plast Reconstr Surg*. 2004;113(4):1229-37. doi:10.1097/01.prs.0000110214.88868.ca
4. Bouhadana G, Aljerian A, Thibaudeau S. The Reconstruction of Plastic Surgery: A Historical Perspective on the Etymology of Plastic and Reconstructive Surgery. *Plast Surg (Oakv)*. 2023;31(4):366-370. doi:10.1177/22925503211064377
5. Peng W, Peng Z, Tang P, et al. Review of Plastic Surgery Biomaterials and Current Progress in Their 3D Manufacturing Technology. *Materials (Basel)*. 2020;13(18):4108. doi:10.3390/ma13184108
6. Marshall CD, Hu MS, Leavitt T, Barnes LA, Lorenz HP, Longaker MT. Cutaneous Scarring: Basic Science, Current Treatments, and Future Directions. *Adv Wound Care (New Rochelle)*. 2018;7(2):29-45. doi:10.1089/wound.2016.0696
7. Lubczyńska A, Garncarczyk A, Wcisło-Dziadecka D. Effectiveness of various methods of manual scar therapy. *Skin Res Technol*. 2023;29(3):e13272. doi:10.1111/srt.13272

ՄԱՇԿԻ ՍՊԻՆԵՐԻ ՎԵՐԼՈՒԾՈՒԹՅՈՒՆ՝ ՆԱԽԱ, ՆԵՐ և ՀԵՏԱԶԳՎԱԾ ՎԻՐԱԲՈՒԺԱԿԱՆ ՆԵՐԱՐԿՄԱՆ ԹԵՐԱՊԻԱՅԻ ՀԵՏ ՓՈՐՁԻ ՄԵՋ

Օլգա Դանիշչուկ,[1] Ալեքսեյ Վոլկով,[2] Վլադիմիր Ռեշետին,[3] Մարինա Դանիշչուկ,[4] Ելենա Կարպովա,[5] Դավիթ Նազարյան[6]

1. Պլաստիկ վիրաբույժ, «Դանիշչուկ կլինիկա» ՍՊԸ-ի գլխավոր բժիշկ, Ռուսաստանի Դաշնության APO FMBA-ի պլաստիկ և էսթետիկ վիրաբուժության բաժանմունքի ասիստենտ
2. Պաթոլոգ, Բժշկական գիտությունների դոկտոր, Ռուս Ուղղափառ Եկեղեցու Մոսկվայի Պատրիարքարանի ANO կենտրոնական կլինիկական հիվանդանոցի ԱՆՕ կենտրոնական կլինիկական

հիվանդանոցի ախտաբանական անատոմիայի ամբիոնի վարիչ, Մոսկվա, ՌԴ
3. Ախտաբան, ախտաբանական անատոմիայի ամբիոնի վարիչ, Ռուսաստանի Դաշնության Մոսկվայի առողջապահության վարչության «Պատերազմի վետերանների թիվ 2 հիվանդանոց» պետական բյուջետային հիմնարկ
4. Մաշկաբան, «Դանիշչուկ կլինիկա» ՍՊԸ-ի գլխավոր տնօրեն, Մոսկվա, ՌԴ
5. Պլաստիկ վիրաբույժ, Ռուսաստանի ազգային գիտահետազոտական բժշկական համալսարանի մաշկային հիվանդությունների և կոսմետոլոգիայի ամբիոնի պրոֆեսոր, դաշնային հետբուհական ուսումնական հաստատություն: Ն.Ի. Պիրոգով, Մոսկվա, ՌԴ
6. Դիմածնոտային վիրաբույժ, բժշկական գիտությունների դոկտոր, Ռուսաստանի APO FMBA պլաստիկ և էսթետիկ վիրաբուժության ամբիոնի պրոֆեսոր, Մոսկվա, Ռուսաստանի Դաշնություն

Ամփոփում

Նպատակ. Ներարկման թերապիայի փորձարարական փորձարկում մաշկի առաջիկա կտրվածքի տարածքում՝ մաշկի սպիացման գործընթացի էսթետիկ տեսքի հասնելու որակը բարելավելու նպատակով:

Նյութեր եւ մեթոդներ. Հետազոտությունն իրականացվել է կրծոսկրի և որովայնի առաջի պատի մաշկի վրա 2 սերտորեն կապված մինի խոզերի վրա: Վիրահատական վիրաբուժական սենյակում 3 սերիա վիրահատությունների համաժամանակ իրականացվել է երկու անձի վրա՝ համապատասխանաբար ուղղանկյունների և տրապեզոիդների տեսքով նախնական հատուկ գծանշումներով, խուլ-արեոլային կոմպլեքսները որպես ուղեցույց են ծառայել ֆիգուրները նկարելու համար: Յուրաքանչյուր փուլում կիրառվել է վիրաբուժական դաշտի նույն տեսակի երկրաչափական գծանշում և կրկնակի միջամտություններ են կատարվել ներարկման թերապիայի և բիոպսիայի նմուշառման միևնույն ոլորտներում: Հետվիրահատական շրջանում՝ 30-րդ և 120-րդ օրերին, վերցվել են բիոպսիայի նմուշներ՝ կլինիկական, ֆոտոմետրիկ և հյուսվածաբանական վերլուծությունների հիման վրա ընթացող վերականգնողական գործընթացները ստուգելու համար:

Արդյունքներ. Նախավիրահատական ներարկման թերապիան նպաստեց նորմալ մաշկին ավելի մոտ կառուցվածքում նորմոտրոֆ սպիի ձևավորմանը՝ համեմատած սպիի նորմալ հյուսվածքների բուժման ժամանակ, ինչը թույլ է տալիս այն առաջարկել նախավիրահատական պատրաստման և մարդկանց հետազոտությունների համար: Ընտրված տեխնիկան թույլ է տալիս գնահատել դասական առաջնային վերքի վերքը՝ ներվիրահատական ֆիզիոլոգիական լուծույթի և բոտուլինի տոքսինի ներդրմամբ և արդյունքների հյուսվածաբանական վերլուծությամբ 1 և 4 ամիս ուշացումով:

Եզրակացություններ. Ներարկման թերապիայի մեթոդը հնարավորություն է տալիս դատել մաշկի գծային սպիի ձևավորման տարբեր մեթոդները ներարկման թերապիայի կիրառմամբ կամ առանց վիրաբուժական հասանելիության, ինչպես նաև համեմատել հյուսվածքների կպչունությունը՝ հյուսվածաբանական վերլուծելով օպտիմալ սպիները: Երբ ձեռք է բերվում ներարկումային BTA թերապիայի արդյունավետությունը, անհրաժեշտ է առանձին ուսումնասիրություն իրականացնել վերքի կափույրների եզրերը կարելիս հյուսվածքային անբավարարության և լարվածության պայմաններում:

АНАЛИЗ РУБЦЕВАНИЯ КОЖИ С ПРЕД-, ИНТРА- И ОТСРОЧЕННОЙ ОПЕРАЦИОННОЙ ИНЪЕКЦИОННОЙ ТЕРАПИЕЙ В ЭКСПЕРИМЕНТЕ

Ольга Данищук,[1] Алексей Волков,[2] Владимир Решетин,[3] Марина Данищук,[4] Елена Карпова,[5] Давид Назарян[6]

1. Врач-пластический хирург, главный врач ООО Клиника Данищука», ассистент кафедры пластической и эстетической хирургии АПО ФМБА Москва, РФ
2. Патологоанатом, доктор медицинских наук, заведующий Отделением патологической анатомии, АНО Центральная клиническая больница Святителя Алексия Митрополита Московского Московской

Патриархии Русской Православной Церкви, Москва, РФ

3. Патологоанатом, заведующий отделением патологической анатомии ГБУЗ «Госпиталь для ветеранов войн № 2» Департамента здравоохранения города Москвы, Москва, РФ
4. Врач-дерматолог, генеральный директор ООО Клиника Данищука», Москва, РФ
5. Врач-пластический хирург, профессор кафедры кожных болезней и косметологии ФДПО РНИМУ им. Н.И. Пирогова, Москва, РФ
6. Врач-челюстно-лицевой хирург, доктор медицинских наук, профессор ассистент кафедры пластической и эстетической хирургии АПО ФМБА России, Москва, РФ

Резюме

Цель: Экспериментальное испытание инъекционной терапии в зоне предстоящего кожного разреза с целью улучшения качества достижения эстетического вида рубцового процесса кожи.

Материалы и методы: Исследование выполнено на кожных покровах грудины и передней брюшной стенки на 2-х близкородственных особях-минипигах. 3 серии операций осуществлялось синхронно на двух особях в условиях хирургической операционной с предварительной специфической разметкой в форме прямоугольников и трапеций соответственно, ориентиром для рисования фигур служили сосково – ареолярные комплексы. На каждом этапе применялась однотипная геометрическая разметка операционного поля и повторные вмешательства выполнялись в тех же зонах инъекционной терапии и забора биоптатов. В послеоперационном периоде на 30 - ые, 120 - ые сутки проводился забор биоптатов для верификации протекающих репаративных процессов на основании клинического, фотометрического и гистологического анализа.

Результаты: Предоперационная инъекционная терапия способствовала формированию нормотрофического рубца по структуре ближе к нормальной коже по сравнению с рубцом при обычном заживлении тканей, что позволяет рекомендовать для предоперационной подготовки и для проведения исследований у людей. Выбранная методика позволяет проводить оценку как классического первичного натяжения раны, с введением физиологического раствора и ботулотоксина интраоперационно и отстрочено в сроки 1 и 4 месяца с гистологическим анализом результатов.

Выводы: Метод инъекционной терапии позволяет судить о разных способах формирования линейного кожного рубца с применением или без применения инъекционной терапией операционного доступа, а также проводить сравнение адгезии тканей гистологически анализируя оптимальное рубцевание. При достижении эффективности инъекционной БТА – терапии, необходимо отдельное исследование в условиях дефицита тканей и натяжения при ушивании краев лоскутов раны.